

DC Stabilizer with Reduced DC Fault Current using Fuzzy Logic Controller for Active Distribution Power System Application

S.NAGA SARANYA¹, P.SUJATHA², P.BHARATH KUMAR³

¹Student, Dept. of Electrical and Electronics Engineering, JNTUA, Anantapur, AP, India.

²Professor, Dept. of Electrical and Electronics Engineering, JNTUA, Anantapur, AP, India.

³Lecturer, Dept. of Electrical and Electronics Engineering, JNTUA, Anantapur, AP, India.

Abstract: *This paper takes a methodical view on the control and security of medium power DC systems in a dynamic appropriation control system considering fault current constraining, system control and converter outline. Lessened terminal capacitance and additional DC impedance are utilized to confine DC fault current and decrease the required converter current rating for medium power DC systems. A versatile DC control stabilizer is proposed to reduce possible system unsteadiness brought by the fault current constraining settings within the sight of constant power load. The impact of the present constraining strategy and the proposed stabilizer on DC fault current and security improvement are approved by simulation with fuzzy logic controller considers utilizing a straight forward two-converter DC circuitry and a multi-terminal DC circuitry in a dynamic conveyance control system and compare the results with PI controller.*

I. INTRODUCTION

DC control system has again turned into an appealing alternative in control transmission and circulation because of expanding power converter infiltrations in current power systems [1]. Present day control gadgets converter based DC control systems can enable conventional AC to control systems to adapt to emerging sustainable power era and Electric Vehicle (EV) issues with more adaptable controllability [2]. A DC control system can likewise profit by less difficult control contrasted with AC systems with no worry on recurrence and receptive power. Besides, DC joins transmit control with no requirement for synchronizing the between associated AC sides [3]. Such elements influence DC to control system a promising answer for associate substantial AC control matrices and reconfigure medium voltage conveyance control systems [4].

With regards to the power dissemination system, DC systems likewise rearrange the incorporation of the standard sustainable eras, photovoltaic and wind turbines for example, in that capacity eras all contain DC joins. On the off chance that these DC joins are associated together alongside stockpiles and DC stacks, a DC microgrid is shaped [5-8]. A typical DC/AC converter in such systems can spare coincidental cost and conceivably offer ascent to bring down change misfortune if most vitality are devoured and put away on the DC side [6]. The idea of the DC microgrid can be stretched out to medium power circulation system with various DC/AC associations with shape a future dynamic appropriation control system [9]. For example, the proposed DC circuitry can be increased up to a few kilometers between weak AC feeders. This makes the system to improve extra AC voltage control capacity and redistribute its moment control flow in a consistent and more ideal path than a hard switch based dynamic conveyance control system without expanding AC fault current[10].

Assurance, and specifically the compelling insurance of the converters after a DC fault because of the releasing of the DC interface capacitors and fault current sustaining from AC side by means of the freewheeling diodes in DC/AC converters is one of the significant worry of present day DC control system[11][12]. Quick acting DC Circuit Breakers (DCCBs), e.g. semiconductor base can viably confine the fault inside a brief period (regularly under 1 ms) however with expanded cost and conduction control misfortune[13]. Then again, mechanical AC and DC Circuit Breakers have insignificant misfortunes and lower cost yet are with moderate breaking reaction, commonly finished a couple of many little seconds[14]. Fault Current Limiting (FCL) procedures are proposed to diminish the peak fault current and its rising rate to encourage circuit breaking. Arrangement impedance infusion is the fundamental thought considered in DC fault current restricting. It can be partitioned into two fundamental sorts: resistive and inductive. Superconductor based procedures are utilized in resistive sort FCL; however they expend significant power amid consistent state operation to keep up superconductivity[15][16]. The other sort is inductive based FCL [17] which can successfully restrain fault current rising rate and lessen top fault current however it doesn't decrease (or may even increment at times) the aggregate releasing vitality amid a DC fault. On the off chance that the DC current and fault vitality can be restricted to enable the converter to survive the fault transient before current interference, AC side breakers or moderate mechanical DCCBs can give a significantly more straightforward and financially savvy arrangement contrasted with the quick DCCB alternative.

Consistent power loads (CPL) can possibly present system unsteadiness in a DC control system. The adjustment of CPLs in a little scale DC organize inside a restricted range has been all around contemplated[18-19]. Including physical resistors were at first proposed however with impressive power misfortunes. Dynamic damping was proposed from that point.

The measure taken for fault current constraining utilizing expanded DC inductance and diminished DC capacitance can additionally worry the unsteadiness issue alongside impressive appropriation length, which has once in a while been examined some time recently. In this paper, a deliberate view on security, soundness control and converter configuration is taken to empower the use of medium power DC system with extensive dispersion length. A versatile stabilizer is proposed to repay neighborhood negative impedance in light of its own nearby location thus no requirement for high data transmission worldwide data obtaining. The proposed versatile control is likewise autonomous from both the consistent power terminal and the network side conditions, and the adaptability of having the capacity to consolidate into CPL terminal control if required.

II. INTRODUCTION TO ACTIVE DISTRIBUTION POWER SYSTEM WITH MVDC NETWORK

With the expanding entrance of inexhaustible era on the circulation control system, the developing discontinuous power could possibly offer ascent to over-voltage or under-voltage at the "last-mile" feeders of a dispersion control system. Medium power DC connections can accordingly be set in the middle of these feeble feeders to enhance their voltage profile and give more adaptable power flow directions as is appeared in Fig 1. As the possible expanding load request of EV charging may stimulate additionally stack crisscrossing, one alternative is to coordinate the charging station (and other sustainable generations) on the DC connect side as appeared in Fig. 1. Along these lines the charging load flow and discontinuous inexhaustible power can be overseen in a more adaptable manner. Such a system could additionally profit by crisis control supply from the accusing station along of sustainable sources when there is a blackout on the AC utility network side.

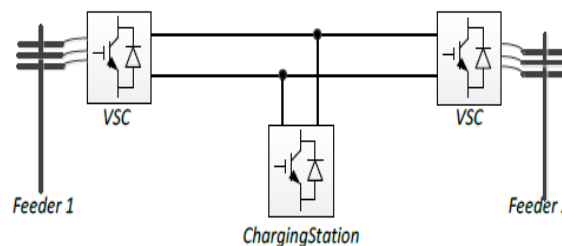


Fig. 1. DC network in an active distribution power system

For a multi-terminal DC arrange inside a dynamic circulation control system, the AC/DC converters might be found some separation far from the heaps including CPL (e.g. charging station) and for prudent reasons existing overhead line ways might be utilized for DC appropriation. Thus, possible DC fault must be considered. Shielding the converters from DC issues and, in the mean time, guaranteeing DC system strength when there is extensive separation between the heaps and AC/DC converters must be managed.

III. DC FAULT AND FAULT CURRENT LIMITING

For medium power DC and dispersion organize applications, two-level VSCs are generally utilized. In this segment, run of the mill DC fault conduct for two-level VSC based medium power DC control systems is examined.

A. DC fault of two-level VSC

In a two-level VSC based DC control system, the most basic fault is DC shaft to-post short, as is appeared by Fig. 2 where C_1 alludes to the terminal capacitance, L_{ac} is the AC reactance, R_1 and L_1 are the terminal impedance at the DC side, V_{dc} is the terminal DC voltage, and i_{LDC} is the present coursing through the DC impedance.

The fault drifters can be for the most part partitioned into three phases as per the dissemination of the overwhelm fault current, which are appeared in Fig. 2. At Stage 1, the primary fault current to a great extent originates from the releasing of the terminal capacitor. At Stage 2, the DC capacitor is completely released and the releasing current, which has come to at its peak esteem, circles through the diodes and continuously rots. At Stage 3, fault current will bolster from the AC side through the AC reactor L_{ac} .

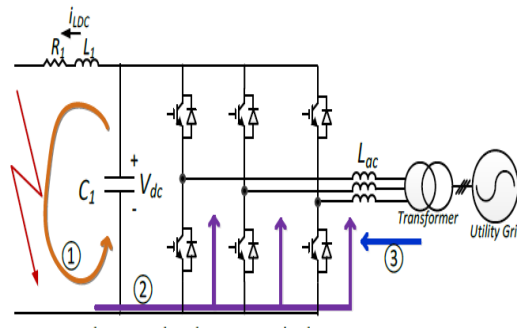


Fig. 2. DC Fault at two-level VSC terminal

At organize 1, expecting all exchanging gadgets have been obstructed, the fault circuit can be displayed as a serial RLC circuit. Expecting the resistance is moderately little for the most pessimistic scenario, the fault current is under-damped and its reaction in time space can be assessed by

$$i_{LDC}(t) = I_{peak} e^{-\alpha t} \sin(\omega_r t + \phi) \quad (1)$$

where I_{peak} is the peak fault current, and α , ω_r , and ϕ are the damping coefficient, reverberation recurrence and beginning edge separately. Accepting the vitality dispersal on the resistance is unimportant at the primary swaying cycle, I_{peak} can be approximated considering the entire exchange of the put away capacitor vitality to the DC inductor toward the finish of Stage 1 as

$$C_1 V_{dc0}^2 / 2 = L_1 I_{peak}^2 / 2 \quad (2)$$

where V_{dc0} is the initial capacitor voltage. Thus,

$$I_{peak} = \sqrt{C_1 / L_1} V_{dc0} \quad (3)$$

As the greater part of the put away vitality in extensive terminal capacitance needs to experience the converter diode amid the fault, it can be deduced from (2) that the decrease of terminal capacitance can adequately lessen vitality coursing through the diodes amid a DC fault. From (3), it can be derived that a littler terminal capacitance and bigger fault inductance can both viably diminish the pinnacle fault current which will flow into the converter diodes in Stage 2. The rising time of the fault current T_r can be assessed by

$$T_r = 2\pi / (4\omega_r) = \sqrt{L_1 C_1} / 4 \quad (4)$$

and the average current rising rate di_{LDC}/dt can be approximated by

$$di_{LDC} / dt = i_{peak} / T_r = V_{dc} / 4L_1 \quad (5)$$

From (5), it can be inferred that the inductance plays a main role in limiting the fault current rising rate.

IV. PRINCIPLES OF THE ADAPTIVE DC POWER STABILIZER

As past depicted, a decreased DC capacitances with additional impedance on the DC terminal can successfully lessen the DC fault current. Be that as it may, such plans can possibly cause system shakiness particularly when associating with a remote consistent power terminal. To handle this issue, a versatile DC control stabilizer is proposed for balancing out the DC control system with little DC capacitance and extra DC terminal impedance.

In this segment, the dynamic impact brought by the additional impedance for DC fault current restricting is investigated first to indicate how the FCL arrangement can weaken system steadiness when there is CPL in operation.

Given a point-to-point DC system as appeared in Fig. 3 (a), the elements of a solitary consistent power terminal is broke down in recurrence space for dynamic and soundness evaluation. Characterizing the DC cut off current I_{peak} for Stage 1 as

$$I_{peak} = DCSCR \times I_{dcn} \quad (6)$$

where $DCSCR$ is the DC short circuit ratio and I_{dcn} is the nominal DC current for the converter, which is defined by

$$I_{dcn} = P_n / V_{dcn} \quad (7)$$

Substituting (6) and (7) into (3) yields

$$DCSCR = \sqrt{C_1 / L_1} V_{dc0} / I_{dcn} \quad (8)$$

Assuming $V_{dc0} = V_{dcn}$ and defining the equivalent nominal resistance R_{dcn} as

$$R_{dcn} = V_{dc} / I_{dcn} \quad (9)$$

there is , $DCSCR = \sqrt{C_1 / L_1} R_{dcn}$ (10)

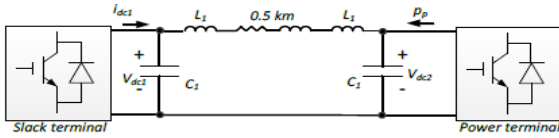


Fig. 3(a) Main circuit of Point-to-Point Medium power DC distribution System

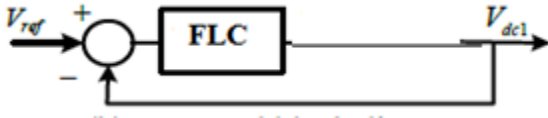


Fig. 3(b) Control block diagram

In a DC control system, bigger consistent power terminal tends to cause swaying when there are substantial DC impedance and little capacitances because of the incited identical negative induction. Accepting the steady power streaming out from the DC arrange is P_p , there is

$$P_p = V_{dcp} I_{dcp} \quad (11)$$

where V_{dcp} is the local DC voltage of the constant power terminal and I_{dcp} is the equivalent DC current. The equivalent small signal resistance R_p can be given by

$$1/R_p = -P_p / V_{dcp}^2 \quad (12)$$

Figs. 3 (a) and (b) demonstrate the disentangled charts of a point-to-point Medium DC control dissemination system and its control, separately. As appeared in Fig. 3 (b), FLC contains $Reg(s)$ and Z_{eq} where, $Reg(s)$ is the slack terminal controller which directs the DC voltage, and $Z_{eq}(s)$ is the proportionate virtual impedance from the slack terminal side. $Reg(s)$ can be communicated as the accompanying:

$$Reg(s) = \frac{(k_p s + k_i) C_1}{(1 + T_s s) s} \quad (13)$$

where k_p and k_i are the proportional and integral gains of the DC voltage PI controller, and T_s is the current loop delay time constant. The equivalent virtual impedance $Z_{eq}(s)$ can be expressed as

$$Z_{eq}(s) = N(s) / D(s) \quad (14)$$

$$N(s) = R_p L C_2 T_p s^3 + (R R_p C_2 T_p + R_p L C_2) s^2 + (R_p T_p + R R_p C_2 + L) s + R_p + R$$

$$D(s) = R_p L C_1 C_2 T_p s^4 + (R R_p C_1 C_2 T_p + R_p L C_1 C_2) s^3 + (R_p C_1 T_p + R R_p C_1 C_2 + L C_1 + R_p C_2 T_p) s^2 + (R_p C_1 + R C_1 + R_1 C_2) s + 1$$

where L and R are the aggregate inductance and resistance between the two terminals, individually. T_p alludes to the power terminal power circle defer time consistent. An option execution is along these lines proposed to utilize a converter that can impersonate the little signal conduct of a latent resistance without resistive power utilization.

To completely counterbalance the negative resistance, there are

$$1/R_v \geq -1/R_p \tag{17}$$

$$1/R_v \geq R_p/V_{dcp}^2 \tag{18}$$

$$1/R_v = 1/R_p + 1/R_v' \tag{19}$$

where R_v is the additional virtual resistance and R_v' is the net resistance subsequent to repaying the negative resistance R_p that can give additional positive damping to the DC terminal. The system setup is exhibited in Fig. 4 (a) where a shunt DC stabilizer is set at the consistent power terminal to effectively mirror the uninvolved resistance. The equal virtual impedance is appeared in Fig. 4 (b). It is conceivable to join the adjustment control into the regular dynamic current control of the CPL terminals if their control systems can be gotten to. As is outlined in Fig. 4 (c), the stabilizer DC current i_{dcs} is changed over to the d-pivot part i_{ds} utilizing the d-hub voltage U_d and is added to the dynamic current reference when d-hub voltage situated control is utilized for the CPL.

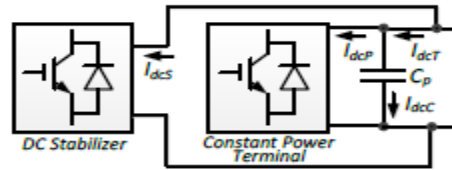


Fig.4(a) Physical DC stabilizer configuration

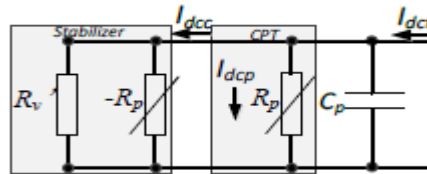


Fig. 4(b) Equivalent virtual impedance

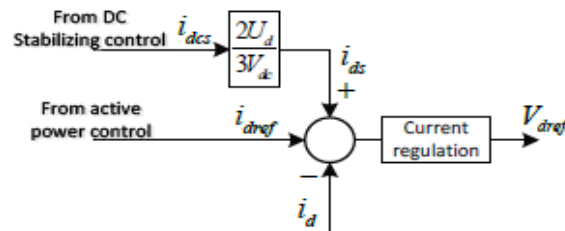


Fig. 4(c) Virtual DC stabilizer circuit

As can be surmised from (12), the power terminal prompts the biggest negative incremental induction while expending the greatest power. In this manner, the virtual resistance is arranged to repay the negative induction comparing to the most extreme power as

$$R_p = -V_{dc}^2/P_{max} \tag{20}$$

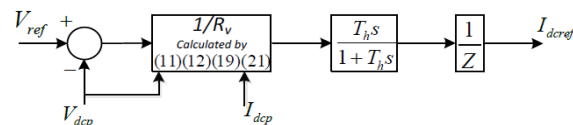


Fig. 5. Adaptive Control of DC Stabilizer

In light of (19) and Fig. 4 (b), the control graph of the proposed versatile conditioner can be appeared , where a first-arrange high-pass channel with a substantial time consistent is added to guarantee a zero normal current amid unflinching state. In Fig. 5, the advanced control and current circle delay is demonstrated as a first-arrange postpone whose time consistent can be equivalent to or bigger than the exchanging cycle of the converter relying upon control usage.

IV FUZZY LOGIC CONTROLLER(FLC)

The Fuzzy Logic Controller(FLC) is one of the most popular controllers due to its logical resemblance to a human operator. The basic principle of FLC is the knowledge base hich in turn depends upon various if then rules,likely to human operator. Unlike other control strategies, this is simpler as there is no complex mathematical knowledge required.

The Fuzzy Logic Toolbox extends the MATLAB technical computing environment with tools for designing systems based on fuzzy logic. The toolbox uses the simple logic rules and then implements these rules in a fuzzy inference system. Alternatively, fuzzy inference blocks are used in Simulink and simulate the fuzzy systems within a comprehensive model of the entire dynamic system.

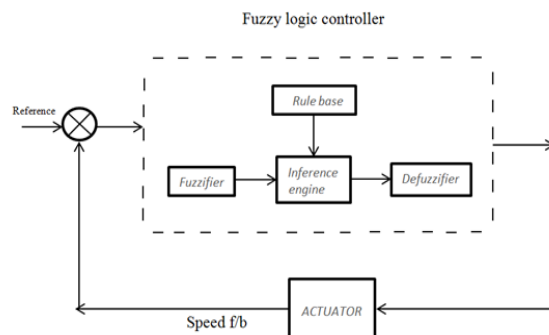


Fig. 6 Structure of Fuzzy Logic Controller

The three variables of the FLC, the error in voltage, the change in error in voltage and the output voltage, have seven triangle membership functions for each. The basic fuzzy sets of membership functions for the variables are as shown in the Figs.6(a),(b),(c). The fuzzy variables are expressed by linguistic variables „positive big(PB)“, „positive medium (PM)“, „positive small (PS)“, „zero (ZE)“, „negative small (NS)“, „negative medium (NM)“, „negative big (NB)“, for all three variables. A rule in the rule base can be expressed in the form: If (e is NB) and (de is NB), then (cd is PB). The rules are set based upon the knowledge of the system and the working of the system. The numbers of rules are 49 for the seven membership functions of the error and the change in error (inputs of the FLC).

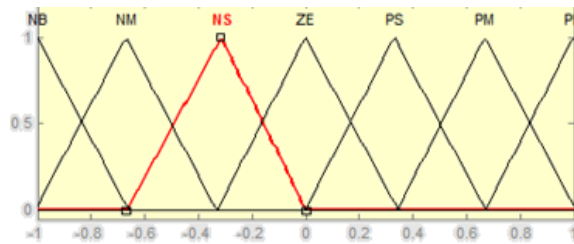


Fig.6(a) : Membership function for error in voltage V_{ref}

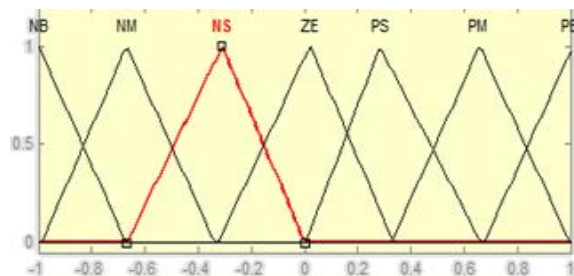


Fig.6(b) : Membership function for change in error for voltage

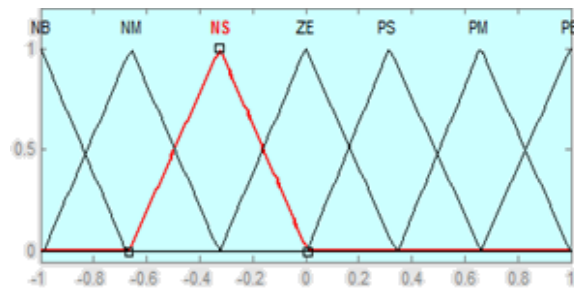


Fig.6(c) : Membership function for output voltage V_{dc1}

Table 1 : Rule base of FLC

$e/\Delta e$	NB	NM	NS	ZE	PS	PM	PB
NB	PB	PB	PB	PM	PM	PS	ZE
NM	PB	PB	PM	PM	PS	ZE	ZE
NS	PB	PM	PS	PS	ZE	NM	NB
ZE	PB	PM	PS	ZE	NS	NM	NB
PS	PM	PS	ZE	NS	NM	NB	NB
PM	PS	ZE	NS	NM	NM	NB	NB
PB	ZE	NS	NM	NM	NM	NB	NB

V. SIMULATION RESULTS OF DC POWER CONDITIONER

A single constant power terminal based DC power network is set up as appeared in Fig. 7. Two-level VSCs and extra DC impedances for additional fault constraining ability are utilized to incorporate the DC system to the AC utility network. One VSC works as the consistent power terminal and the other is the slack terminal controlling the DC voltage. The separation between the two converters is 2 km. A little DC-DC converter with supercapacitor based vitality stockpiling system (ESS) is put at the consistent power terminal side as the power stabilizer. The consistent power terminal current i_{PT} , slack terminal current i_{ST} and the power conditioner terminal i_{ESS} are characterized alongside the DC voltage of the slack terminal V_{ST} and with VPT as it needs.

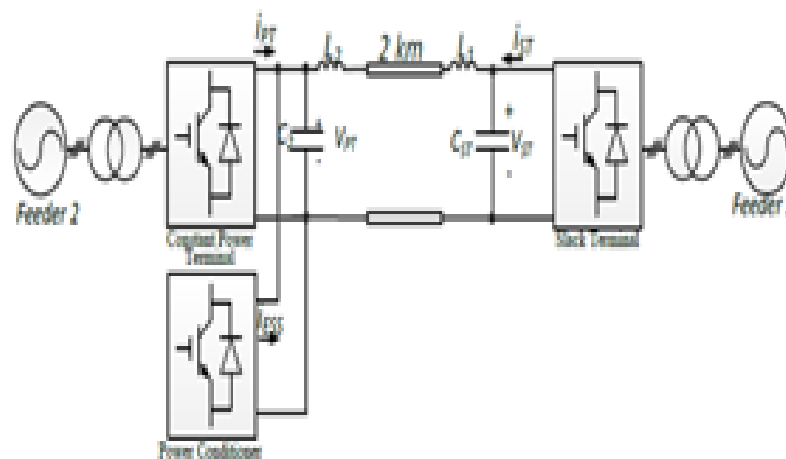


Fig.7. Sample system with single power terminal and conditioner

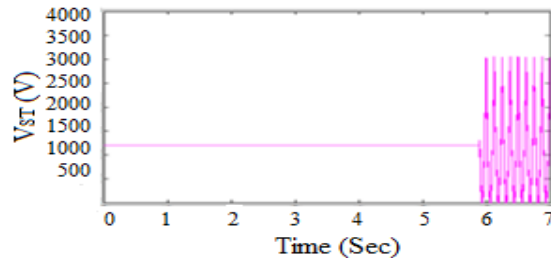


Fig.8(a) shows oscillations in DC voltage of Slack Terminal V_{ST} with time

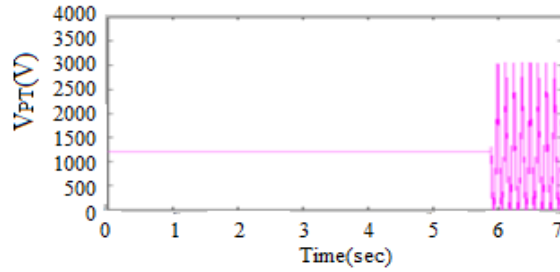


Fig.8(b) shows oscillations in DC voltage of Power Terminal V_{PT} with time

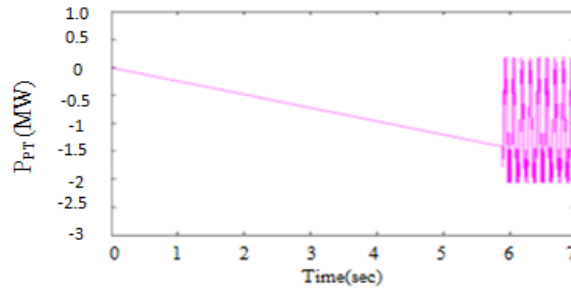


Fig.8(c) shows oscillations in power at the Power Terminal P_{PT} with time

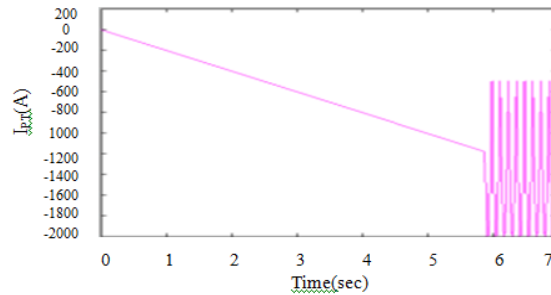


Fig.8(d) shows the oscillations in constant Power Terminal current i_{PT} with time

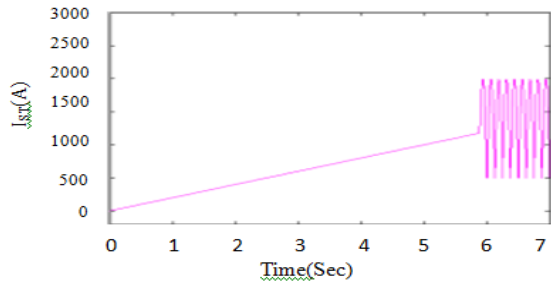


Fig.8(e) shows the oscillations in constant Slack Terminal current i_{ST} with time

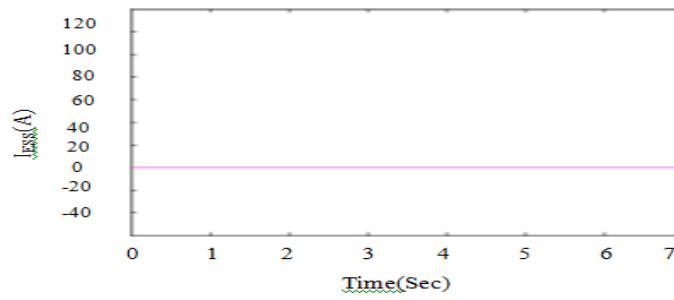


Fig.8(f) shows current in Energy Storage System(ESS) placed at constant power terminal as the power stabilizer

The simulation results in Fig.8 shows that the system is tested without power stabilizer with a defined power ramp of 0.2MW/s from the constant power terminal.

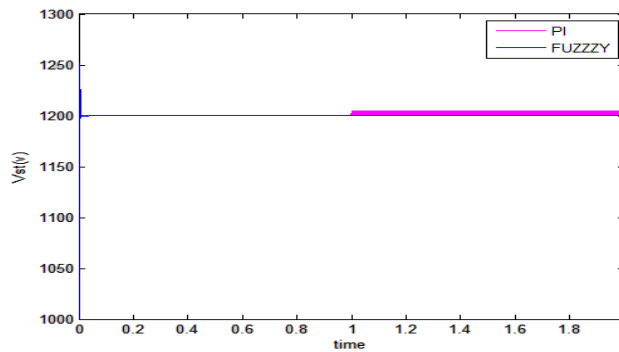


Fig.9(a) shows the DC voltage of Slack Terminal V_{ST} with time

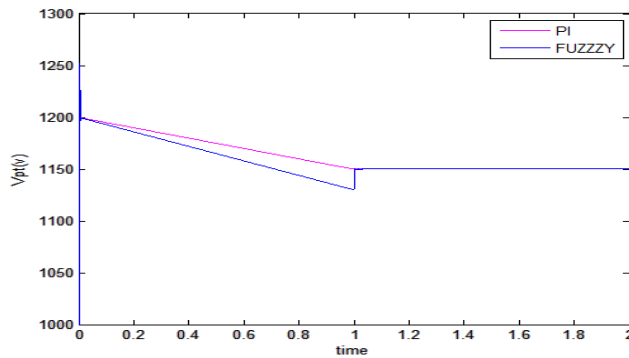


Fig.9(b) shows the DC voltage of Power Terminal V_{PT} with time

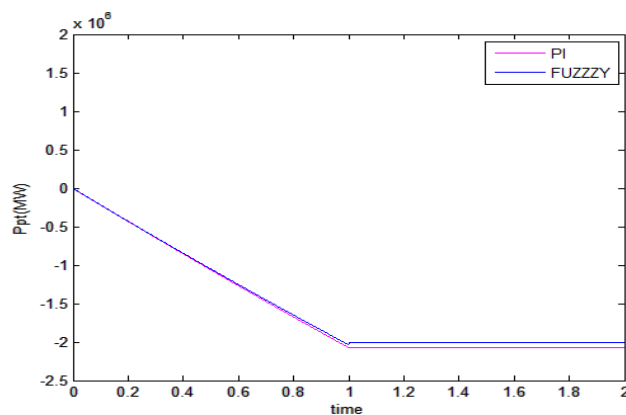


Fig.9(c) shows the power at the Power Terminal P_{PT} with time

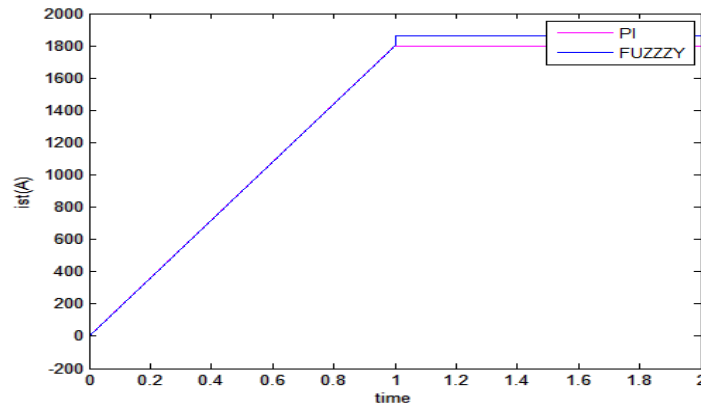


Fig.9(d) shows the constant Slack Terminal current i_{ST} with time

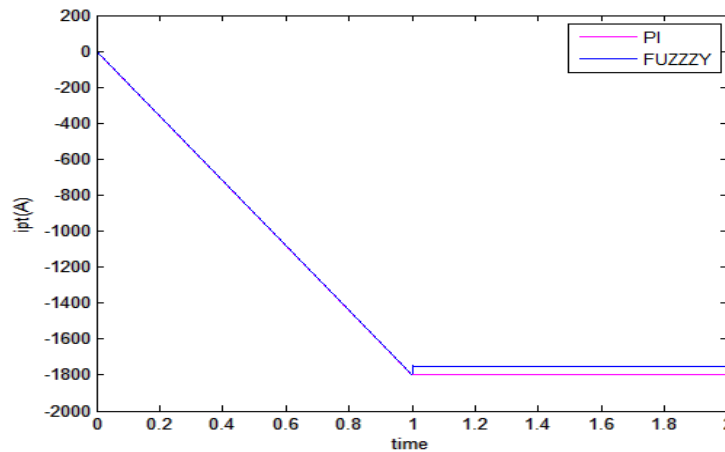


Fig.9(e) shows the constant Power Terminal i_{PT} with time

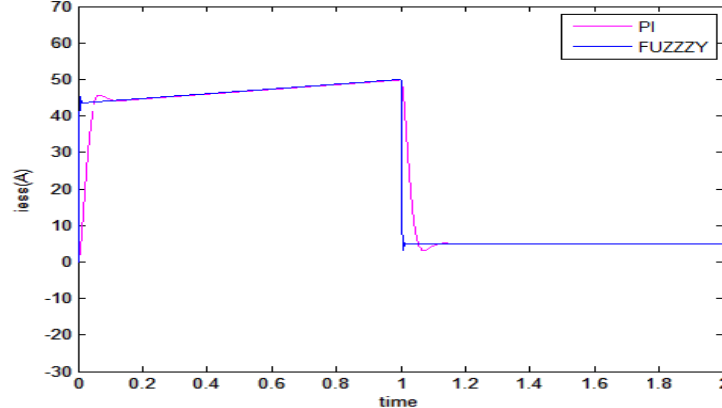


Fig.9(f) shows the Power stabilizer consumes current with time

The Fig.9 shows the comparison between PI controller and Fuzzy Logic Controller when the DC stabilizer is activated. The power stabilizer only consumes 50 A at its peak, which is less than 3% of the rated current of the constant power terminal and gradually drops to zero after the ramp indicating only a small energy and power rating is required for the storage.

VI. APPLICATION OF MVDC NETWORK WITHIN AN ACTIVE DISTRIBUTION NETWORK

A virtual DC stabilizer is joined inside the available consistent power terminal side (i.e. VSC 6) as appeared by the specked chart in Fig. 10 and a genuine DC stabilizer is introduced at the difficult to reach control terminal of the charging station in Fig. 8. All the DC terminals are outlined with additional fault breaking point ability and the charging station is thought to have the capacity to disengage the DC fault current with galvanic confined topology.

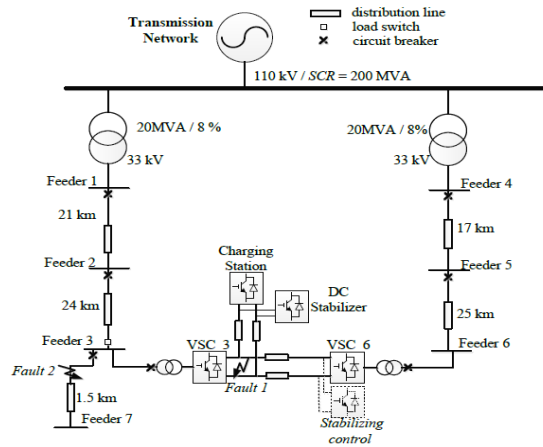


Fig.10. Active distribution power system configuration

Table 2 : Parameters of Distribution Network

Nominal Voltage and Ratings	
Distribution nominal voltage	33kV
Transmission nominal voltage	110kV
Transmission short circuit rating	200kVA
Transformer power rating	20MVA
Primary inductance	0.04 p.u.
Secondary inductance	0.04 p.u.
AC distribution impedance	0.136 Ω/km, 0.356 mH/km and 0.262 nF/km
Feeder Load	
Feeder 1	0.15+j0.05 p.u.
Feeder 2	0.5+j0.05 p.u.
Feeder 3	0.05+j0.01 p.u.
Feeder 4	-0.1+j0.01 p.u.
Feeder 5	-0.25j0.01 p.u.
Feeder 6	-0.05+j0.01 p.u.
Feeder 7	0.005+j0.001 p.u.

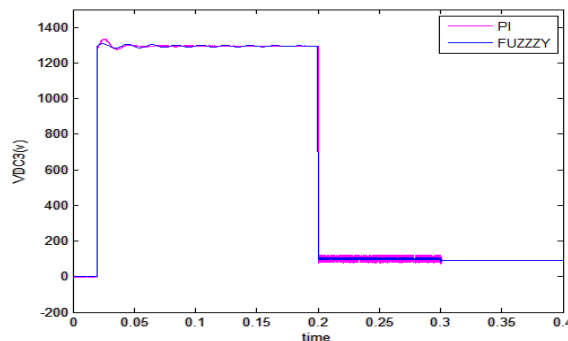


Fig.11(a) The DC Voltage V_{DC3} at VSC3 which connects to feeder 3

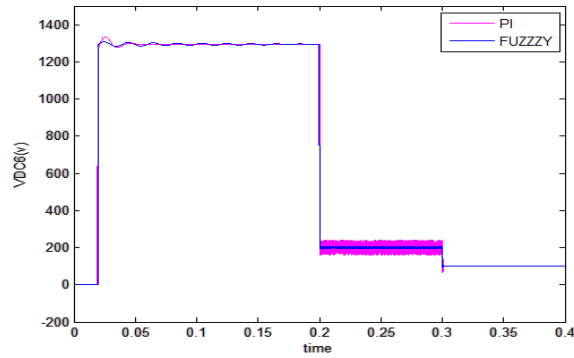


Fig.11(b) The DC Voltage V_{DC6} at VSC6 which connects to feeder 6

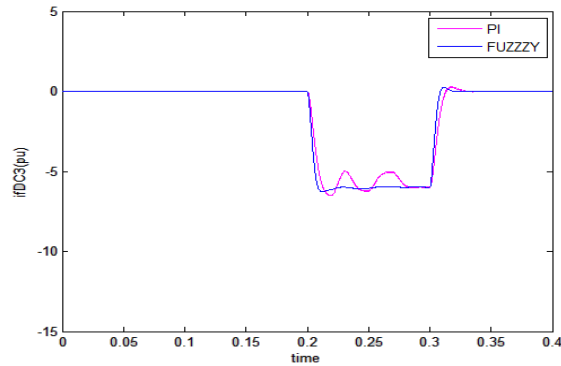


Fig.11(c) The fault current behaviour I_{fDC3} at feeder 3

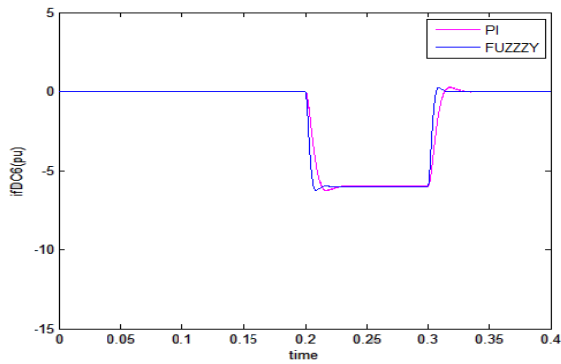


Fig.11(d) The fault current behaviour I_{fDC6} at feeder 6

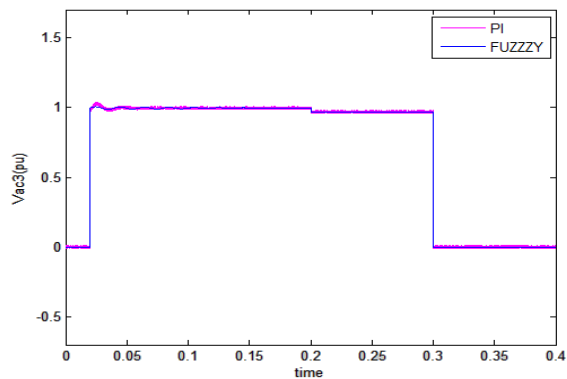


Fig.11(e) AC Voltage V_{AC3} at feeder3

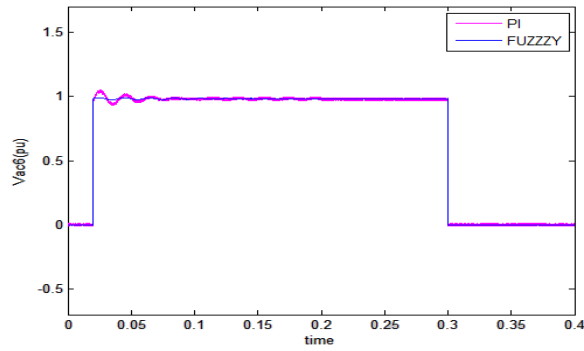


Fig.11(f) AC Voltage V_{AC6} at feeder6

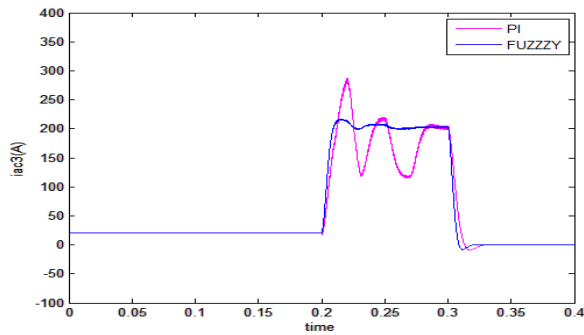


Fig.11(g) AC fault Current behaviour I_{fAC3} at feeder 3

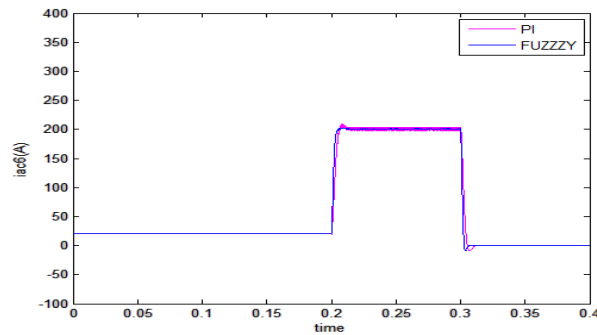


Fig.11(h) AC fault behaviour I_{fAC6} at feeder6

Fig.11 shows the DC fault behavior at VSC 3 (Fault 1) which is connected to feeder 3. The system imports a ramp power of 0.25MW/s to the DC network at VSC6. When the DC fault occurs, both DC voltages at VSC3 and VSC6 falls to zero and the DC fault currents I_{fDC3} (at VSC3) and I_{fDC6} (at VSC6) increases. The corresponding AC side fault currents I_{fAC3} and I_{fAC6} also increases.

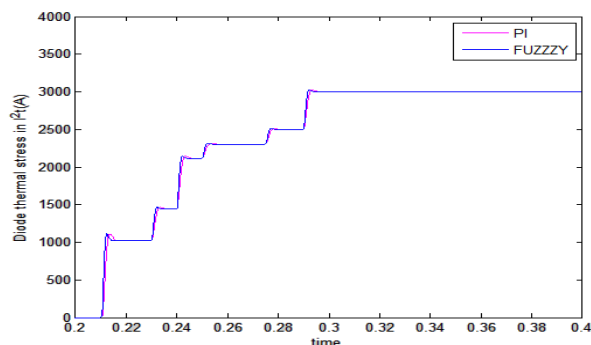


Fig.11(i) Diode thermal stress in I^2t

The converter IGBTs are blocked after the fault, the VSC fault current goes through the diodes. The diodes accumulated I^2t during transient is a good indicator for considering their transient overload capability. The accumulated I^2t of diode is shown in Fig.11(i) which increases till current interruption after the fault.

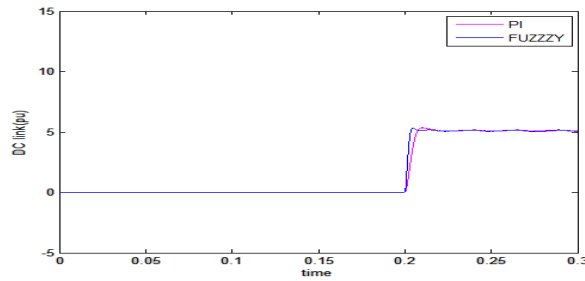


Fig. 12(a) AC fault current at feeder7(fault 2) by using DC links

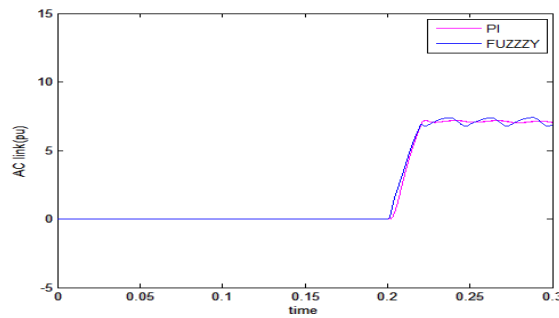


Fig.12 (b) AC fault current at Feeder 7 (Fault 2) by using AC links

From the Fig.12(a) & 12(b), it is better to use DC link over the AC link, as it does not reduce the equivalent short circuit impedance.

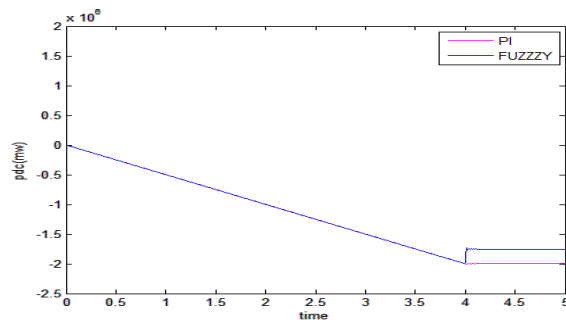


Fig.13(a) Single stabilizer performance with ramp charging load, P_{DC3} : Power consumed by VSC3

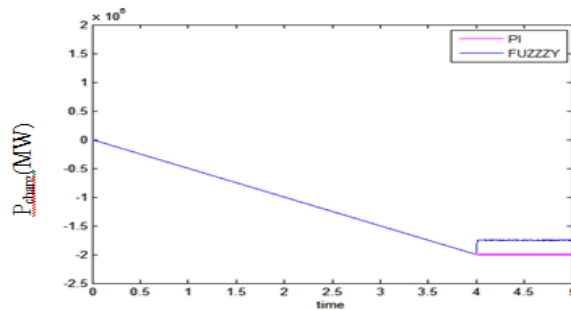


Fig.13(b) P_{charge} : Power discharged from the charging station

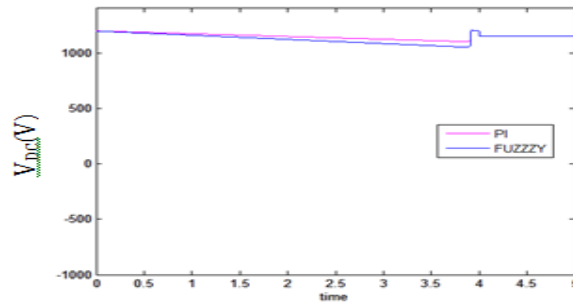


Fig.13(c) V_{DC} : DC voltage at the charging station bus

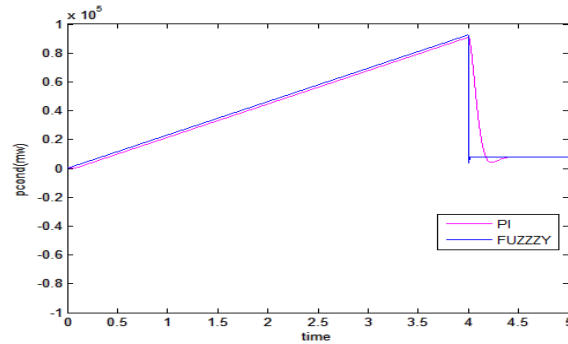


Fig.13(d) P_{cond} : power discharged by the DC stabilizer

Fig.13 shows the performance when the charging side stabilizer is activated. The stabilizing power gradually increases, since the stabilizer function provides dynamic response due to addition of high pass filter.

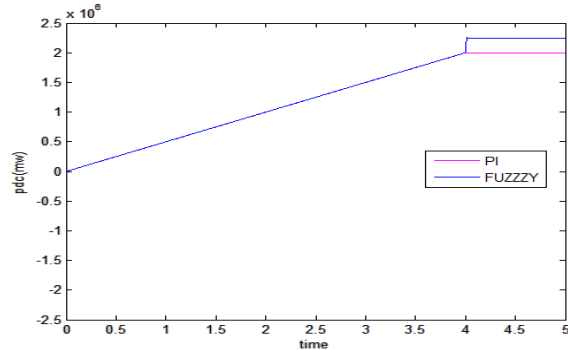


Fig.14(a) Dual stabilizer performance with power ramp at VSC6, P_{DC6} : Power consumed by VSC6.

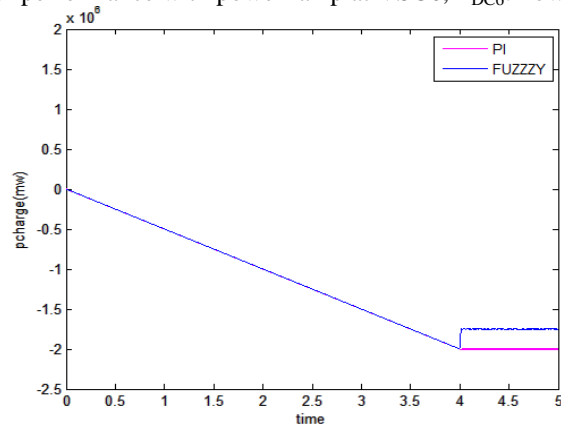


Fig.14(b) P_{charg} : Power discharged from the charging station

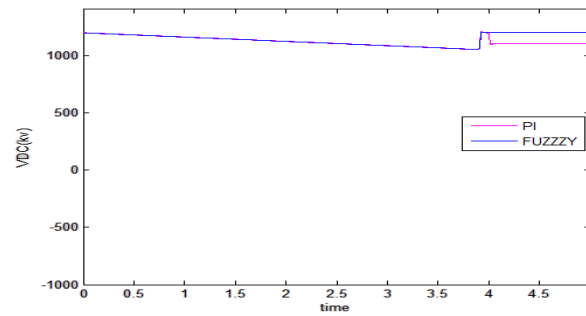


Fig.14(c) V_{DC} : DC voltage at the charging station bus

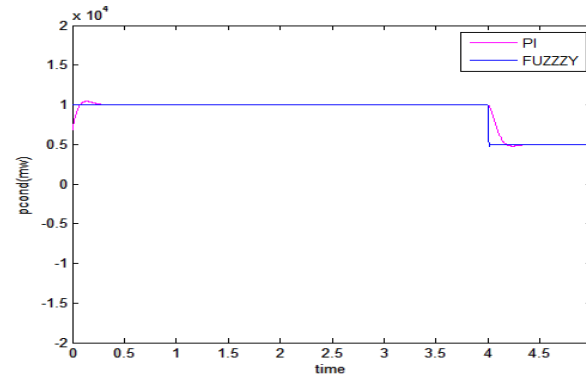


Fig.14(d) P_{cond} : Power discharged by the stabilizer

When the stabilizing control is activated the oscillation is eliminated and the system is completely stable across the whole power range.

VII. CONCLUSION

In this paper, a medium power DC system solution considering DC fault current limiting and stability for active distribution power system has been investigated. By replacing the normal open switch with a DC link, the distribution network achieves improved power distribution control and load ability without increasing AC fault current.

To overcome the effect of distortions in PI controller with charging stabilizer, Fuzzy logic Controller (FLC) is proposed. Unlike other control strategies, this is simpler as there is no complex mathematical knowledge is required. The error in voltage, change in error and output voltage are the basic fuzzy sets of membership functions, which have seven triangle membership functions for each are shown. The rulebase for FLC is shown in the tabulation. The FLC provides better steady state stability conditions when compared to PI controller. Hence, the proposed stabilizer on DC fault current and security improvement are approved by simulation with FLC. The fuzzy systems within a comprehensive model of the entire dynamic system is simulated and the results are compared with PI controller.

REFERENCES

- [1] K. Kurohane, T. Senjyu, A. Uehara, A. Yona, T. Funabashi and Chul-Hwan Kim, "A hybrid smart AC/DC power system," in Proc. 2010 the 5th IEEE Conference on Industrial Electronics and Applications (ICIEA), pp.764-769, 15-17 June 2010
- [2] P. Goli and W. Shireen, "PV integrated smart charging of PHEVs based on DC link voltage sensing," *IEEE Trans. Smart Grid*, vol. 5, no. 3, pp.1421 -1428, 2014
- [3] J. Yu, M. Xiao and G. G. Karady, "Dynamic Performance of Embedded HVDC with Frequency Control Strategy," in Proc. 2015 the Power and Energy Society General Meeting (PESGM), 2015
- [4] J. Alcala,; V. Cardenas, J. Perez-Ramirez,; R.J. Betancourt, H. Miranda, "Improving power flow in transformers using a BTB converter to balance low voltage feeders," in Proc. 2012 IEEE Energy Conversion Congress and Exposition (ECCE), pp.2038-2044, 15-20 Sept. 2012
- [5] H. Kakigano, Y. Miura and T. Ise, "Low-voltage bipolar-type dc microgrid for super high quality distribution", *IEEE Trans. Power Electron.*, vol. 25, no. 12, pp.3066 -3075, 2010

- [6] D. Salomonsson, L. Soder and A. Sannino, "An adaptive control system for a dc microgrid for data centers", *IEEE Trans. Ind. Appl.*, vol. 44, no. 6, pp.1910 -1917, 2008
- [7] D. Chen and L. Xu, "Autonomous dc voltage control of a dc microgrid with multiple slack terminals", *IEEE Trans. Power Syst.*, vol. 27, no. 4, pp.1897 -1905, 2012
- [8] X. Lu, J. Guerrero, K. Sun and J. Vasquez "An improved droop control method for dc microgrids based on low bandwidth communication with dc bus voltage restoration and enhanced current sharing accuracy", *IEEE Trans. Power Electron.*, vol. 29, no. 4, pp.1800 -1812, 2014
- [9] M. Barragan, J.M. Mauricio, A. Marano, M. Nieves, J. Churio, J.M. Maza-Ortega, E. Romero and A. Gomez, "Operational benefits of multiterminal DC-links in active distribution networks," in *Proc. 2012 IEEE Power and Energy Society General Meeting*, 22-26 July 2012
- [10] M. E. Baran and F. F. Wu, "Network reconfiguration in distribution system for loss reduction and load balancing", *IEEE Trans. Power Del.*, vol. 4, no. 2, pp.1401 -1407, 1989
- [11] D. Salomonsson, L. Soder and A. Sannino, "Protection of low-voltage DC microgrids", *IEEE Trans. Power Del.*, vol. 24, no. 3, pp.1045 -1053, 2009
- [12] S. D. A. Fletcher , P. J. Norman , S. J. Galloway , P. Crolla and G. M. Burt "Optimizing the roles of unit and non-unit protection methods within dc microgrids", *IEEE Trans. Smart Grid*, vol. 3, no. 4, pp.2079 -2087, 2012
- [13] K. Sano and M. Takasaki "A surgeless solid-state DC circuit breaker for voltage-source-converter-based HVDC systems", *IEEE Trans. Ind. Appl.*, vol. 50, no. 4, pp.2690 -2699, 2013
- [14] M. Noe and M. Steurer, "High-temperature superconductor fault current limiters: Concepts, applications, and development status," *Supercond. Sci. Technol*, vol. 20, pp. R15–R29, Mar. 2007.
- [15] C. Schacherer, J. Langston, M. Steurer, and M. Noe, "Power hardware- in-the-loop testing of a YBCO coated conductor fault current limiting module," *IEEE Trans. Appl. Supercond.*, vol. 19, no. 3, pp.1801–1805, Jun. 2009.
- [16] C.M. Frank, "HVDC Circuit Breaker: A Review Identify Future Research Needs," *IEEE Trans. Power Del.*, vol. 26, no. 2, pp. 998–1007, Dec. 2007.
- [17] M. Cespedes, L. Xing, and J. Sun, "Constant-power load system stabilization by passive damping," *IEEE Trans. Smart Grid*, vol. 26, no. 7, pp. 1832-1836, Jul. 2011.
- [18] W. Du, J. Zhang, Y. Zhang and Z. Qian, "Stability Criterion for Cascaded System With Constant Power Load," *IEEE Trans. Power Electron.*, vol. 28, no. 4, pp. 1843–1851, Apr. 2013.
- [19] Dong Chen and Lie Xu, "Adaptive DC stabilizer with reduced fault current for Active Distribution Power System Application," *IEEE Trans. On Power Systems*, volume: 32, issue : 2, pp: 1430-1439, Year 2017.